Journal of Theoretical Biology 517 (2021) 110596

Contents lists available at ScienceDirect

Journal of Theoretical Biology

journal homepage: www.elsevier.com/locate/yjtbi

Coordination of local and long range signaling modulates developmental patterning

Carly Williamson [a], Helen M. Chamberlin [b], Adriana T. Dawes [a,b,*]

[a] Department of Mathematics, The Ohio State University, Columbus, OH 43210, United States
[b] Department of Molecular Genetics, The Ohio State University, Columbus, OH 43210, United States

ARTICLE INFO

Article history:
Received 2 July 2020
Revised 18 December 2020
Accepted 13 January 2021
Available online 26 January 2021

2010 MSC:
92C15

Keywords:
Developmental biology
Differential equations
Biological patterns

ABSTRACT

The development of multicellular organisms relies on correct patterns of cell fates to produce functional tissues in the mature organism. A commonly observed developmental pattern consists of alternating cell fates, where neighboring cells take on distinct cell fates characterized by contrasting gene and protein expression levels, and this cell fate pattern repeats over two or more cells. The patterns produced by these fate decisions are regulated by a small number of highly conserved signaling networks, some of which are mediated by long range diffusible signals and others mediated by local contact-dependent signals. However, it is not completely understood how local and long range signals associated with these networks interact to produce fate patterns that are both robust and flexible. Here we analyze mathematical models to investigate the patterning of cell fates in an array of cells, focusing on a two cell repeating pattern. Bifurcation analysis of a multicellular ODE model, where we consider the cells as discrete compartments, suggests that cells must balance sensitivity to external signals with robustness to perturbations. To focus on the patterning dynamics close to the bifurcation point, we derive a continuum PDE model that integrates local and long range signaling. For those cells with dynamics close to the bifurcation point, sensitivity to long range signals determines how far a pattern extends in space, while the number of local signaling connections determines the type of pattern produced. This investigation provides a general framework for understanding developmental patterning, and how both long range and local signals play a role in generating features observed across biology, such as species differences in nematode vulval development and insect bristle patterning, as well as medically relevant processes such as control of stem cell fate in the intestinal crypt.

1. Introduction

Cells in multicellular organisms exhibit a variety of "fate" or "type" patterns. For example, blood vessels reproducibly branch into tissue, digits emerge in a distinct pattern across a developing limb bud, and bristles form in particular arrays on the cuticle of an insect (Herbert and Stainier, 2011; Sonnen et al., 2018; Simpson et al., 1999). These and most other biological patterns are established through coordinated communication among the participating cells, mediated by protein or chemical signals. Signals that establish patterns include local (neighbor-to-neighbor) signals, such as the Notch receptor and its set of membrane-bound ligands, and longer-range (diffusible) signals that typically emerge from a source and exhibit a gradation across a space of many cell diameters. While a variety of mathematical investigations have explored the properties of these two types of signaling processes, including (De Back et al., 2013; Fisher et al., 2005; Irons et al., 2010; O'Dea and King, 2012; Giurumescu, 2006), it is clear that many cellular patterns result from the coordination of both local and long-range processes and therefore the dynamics of these biological systems are not fully captured by these single-feature analyses. To address this gap, we sought to systematically investigate the relationship between different types of signals and their potential to impact cell fate patterns using simplified systems of ordinary and partial differential equation models.

Short-range signals such as those mediated by Notch are important in establishing binary cell fate choice, such as in "lateral inhibition" where neighboring cells interact to adopt fates that are distinct from each other (Erkenbrack, 2018; Tiedemann et al., 2017; Sternberg, 1988; Fig. 1). Experimental studies in a range of

* Corresponding author at: Department of Mathematics, The Ohio State University, Columbus, OH 43210, United States.
E-mail address: dawes.33@osu.edu (A.T. Dawes).

https://doi.org/10.1016/j.jtbi.2021.110596
0022-5193/

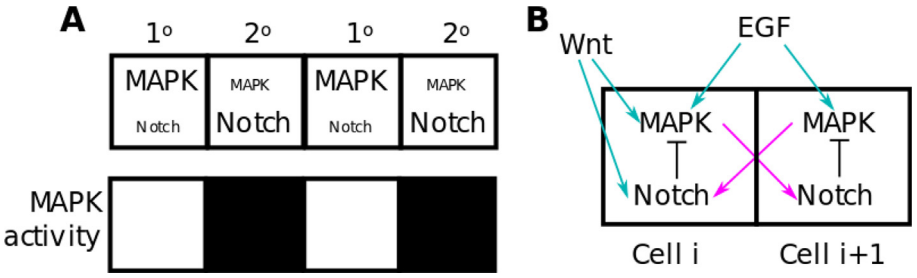

Fig. 1. Schematic of alternating cell fate pattern and simplified MAPK/Notch signaling network. A. Alternating cell fates, characterized by reciprocal signaling pathway activity, are a common patterning mechanism during development. Motivated by alternating cell fates of the egg laying structure (vulva) of developing nematode worms, we designate a primary (1°, white) cell as having high MAPK signaling pathway activity/low Notch pathway activity, and a secondary (2°, black) cell as having low MAPK/high Notch pathway activity. The alternating cell fates can be represented as a discrete array of cells (bottom). B. Simplified signaling network under study. High MAPK activity enhances Notch pathway activity in neighboring cells via local contact-mediated signaling (magenta arrows), while Notch activity inhibits MAPK activity within the same cell (black blunt end arrows). EGF and Wnt (cyan arrows) are external diffusible signals which act to promote MAPK or MAPK and Notch pathway activity, respectively.

organisms demonstrate that this local process can be modulated by diffusible signals including FGF, EGF, Wnt, or TGFβ (Pandey et al., 2019; Romero-Carvajal et al., 2015; Sternberg, 2005; Beumer and Clevers, 2016). These signals activate intracellular pathways that include the MAP kinase cascade (MAPK) and Notch. To implement our analysis, we have selected the process of vulval development in *Caenorhabditis* nematodes as a specific biological example in which two long-range signals (Wnt and EGF) and one local signal (Notch) function to establish a pattern of alternating cell fates (Fig. 1).

The vulva acts as the egg laying structure in nematode worms, and is the passage through which embryos are expelled from the adult worm. See Sternberg (2005) for a comprehensive review of vulval development. In brief, the vulva is generated from six cells, the vulval precursor cells (VPCs), that align in a single row in the ventral epidermis. The anchor cell, which is positioned above the VPCs, is the source of the long range diffusible EGF and one of the sources of the Wnt signal. The VPCs take on one of three specific fates in response to the EGF and Wnt signals, as well as contact-mediated Notch signaling to neighboring VPCs. The primary (1°) cell fate is characterized by high MAPK activity/low Notch activity and a secondary (2°) cell fate is characterized by low MAPK/high Notch activity. The tertiary (3°) cell fate is characterized by low MAPK/low Notch activity. High MAPK activity induced by long range EGF and Wnt signals enhances Notch pathway activity in neighboring cells, while high Notch activity inhibits MAPK activity (Fig. 1), resulting in alternating 1° and 2° cell fates. The cells that take on 1° and 2° fates proceed through a series of divisions to form the sides and top of the vaulted vulval structure. The 3° cells divide only a single time and are absorbed into the epidermis. The alternating pattern of cell fates induced by EGF, Wnt and Notch signaling is critical for proper construction of this organ (Sternberg, 2005; Myers and Greenwald, 2007). In certain mutants that enhance MAPK activity, a pattern of alternating 1° and 2° cell fates is commonly observed across all six VPCs (Sternberg and Horvitz, 1989; Han et al., 1990).

Using a combination of bifurcation analysis with a multicellular ODE model and a continuum PDE that approximates the dynamics close to the bifurcation point, we demonstrate how modulations to long range signals can render the network more or less robust to perturbation, which are features observed when comparing fate patterning in different *Caenorhabditis* species. We also show how the interplay between local and long range signaling allows cells in 1D or 2D tissues to control both the type and spatial extent of patterning. These results indicate how local and long range signaling contribute equally important but distinct functions during the patterning of a developing tissue, and how modulation of their input can lead to different patterning outcomes. While we focus on the alternating pattern of cell fates observed in vulval development of *Caenorhabditis* species, the general nature of this investigation can shed light into other alternating patterns observed during development that rely on a combination of local and long range signaling.

2. Methods

2.1. Spatially discrete two cell and multicellular model

In this model, each cell is treated as a discrete, well-mixed compartment. Cells communicate with each other via a local signal (Notch), and receive two external, long-range signals that are important for, and modulate, the intercellular interaction (EGF, Wnt) in a manner consistent with experimental evidence (Sternberg, 2005). As described above, a key inductive signal (EGF) activates a target within a cell (MAPK) that initiates the "lateral inhibition" on the neighboring cell. The second external signal (Wnt) modulates the response to each target (MAPK and Notch; Fig. 1). While the relationship among these specific pathways inspires the analysis, similar relationships among long range and local signals are observed in a number of biological processes. Consequently, while we use these gene names to identify model variables for convenience, the analyses and conclusions in this study are not limited to processes only involving these three signaling pathways.

The simplified network of interactions shown in Fig. 1 is modeled in a discrete array of cells by the following dimensional equations:

$$\text{Notch activity}: \quad \frac{d\eta_i}{d\tau} = k_{WN} W_i F(\bar{\xi}) - k_N \eta_i \tag{1}$$

$$\text{MAPK activity}: \quad \frac{d\xi_i}{d\tau} = (k_{EM} E_i + k_{WM} W_i) G(\eta_i) - k_M \xi_i \tag{2}$$

As detailed in the Supplementary Information (Section S1), the equations can be nondimensionalized to yield the following system of ODEs:

$$\text{Notch activity}: \quad \frac{dN_i}{dt} = W_i f(\bar{M}_i) - N_i \tag{3}$$

$$\text{MAPK activity}: \quad \frac{dM_i}{dt} = \gamma(\lambda_i g(N_i) - M_i) \tag{4}$$

where $i = 1, 2, \ldots$ corresponds to the cell index, and $\lambda_i = \frac{E_i + \mu W_i}{\mu + 1}$.

Variable and parameter names and meanings are listed in Tables S1 and S2. The bar superscript denotes the average activity from neighboring cells: $\bar{M}_i = \frac{1}{\nu}\sum_{j=1}^{\nu} M_j$, where j runs over all ν nearest neighbors of cell i. Following a similar model (Collier et al., 1996; O'Dea and King, 2011, 2012), we choose the following Michaelis–Menten functions to represent coupling between cells:

$$f(\sigma) = \frac{\sigma^k}{\alpha + \sigma^k}, \tag{5}$$

$$g(\sigma) = \frac{1}{1 + \beta\sigma^h}, \tag{6}$$

where f is a monotonically increasing function representing the increase in Notch activity in response to increased MAPK activity in neighboring cells, while g is a monotonically decreasing function representing the inhibitory effect of Notch on MAPK activity in the same cell. The magnitude of local coupling is represented by the parameter k_{WN} in the dimensional model, which is incorporated into the parameter β of Eq. (6) in the nondimensionalized model. Further details of the nondimensionalization can be found in the Supplementary Information (Section S1).

For the case where there is no local coupling between neighboring cells, the nondimensionalized model is:

$$N_i(0) = 0 \tag{7}$$

$$\frac{dM_i}{dt} = \gamma(\lambda_i - M_i) \tag{8}$$

In the absence of local coupling, the Notch pathway is not activated and there is no inhibition of MAPK activity by the long range EGF signal. This loss of Notch activity in the absence of local coupling is consistent with experimental evidence: when the Notch receptor is nonfunctional, neighboring VPCs in the developing nematode vulva take on primary cell fates with high MAPK activity instead of the usual high MAPK/high Notch activity in alternating cells observed during normal development (Greenwald et al., 1983). See Supplementary Information for details of the nondimensionalization.

2.2. Continuum multicellular PDE model

To investigate patterning dynamics close to the bifurcation point, we derive a continuum PDE model that explicitly incorporates both local and long range signaling, following a similar procedure as O'Dea and King (2011, 2012). In particular, we wish to understand how small changes in local or long range signaling can influence the type and extent of patterning across an array of cells. Derivation details can be found in the Supplementary Information (Section S4).

1D Continuum PDE: In the presence of local coupling between two neighboring cells in a 1D array of cells, we expand the long range EGF and Wnt signals as:

$$\begin{aligned} E &= e + \delta^2 E(x) \\ W &= w + \delta^2 W(x) \end{aligned}$$

where e, w denote the bifurcation values of EGF and Wnt, respectively, and $\delta \ll 1$ denotes cell size. As in O'Dea and King (2011, 2012), the spatial scale is represented by $x = \delta i$, where i is the cell index. The expansion of E and W is of order δ^2 to reflect the spatial scale of diffusion-mediated decay and for notational simplicity. This expansion leads to:

$$\begin{aligned} \lambda &= \Lambda + \delta^2\lambda(x) \\ &= \tfrac{e+\mu w}{\mu+1} + \tfrac{\delta^2(E(x)+\mu W(x))}{\mu+1} \end{aligned}$$

In the presence of local signaling, there is a pitchfork bifurcation leading to an alternating pattern, so we denote MAPK and Notch activity in odd numbered cells as $M^+(x,t)$, $N^+(x,t)$, and in even cells as $M^-(x,t)$, $N^-(x,t)$. As detailed in the Supplementary Information (Section S4), the resulting PDE for Notch activity in odd numbered cells is given by:

$$\rho\frac{\partial N_1^+}{\partial \tau} = \frac{\partial^2 N_1^+}{\partial x^2} - \phi N_1^+ - \psi\left(N_1^+\right)^3 \tag{9}$$

where

$$\rho = 2\left(\frac{1}{\gamma} + 1\right) \tag{10}$$

$$\begin{aligned} \phi(x) = \Lambda w\Big(&\lambda(x)g(N^*)\Big(f''(M^*)g'(N^*) + f'(M^*)^2 g''(N^*)w\Big) \\ &+ W(x)f(M^*)\Big(f'(M^*)g''(N^*) + f''(M^*)g'(N^*)^2\Lambda\Big)\Big) \\ &- 2\frac{\lambda(x)}{\Lambda} - 2\frac{W(x)}{w} \end{aligned} \tag{11}$$

$$\begin{aligned} \psi = \Lambda w\Bigg(&\frac{f'(M^*)g'''(N^*) + f'''(M^*)g'(N^*)^3\Lambda^2}{3} \\ &+ \frac{f'(M^*)^2 g''(N^*)^2\Lambda + f''(M^*)^2 g'(N^*)^4\Lambda^3 w}{2}\Bigg) \end{aligned} \tag{12}$$

Notch activity in even numbered cells and MAPK activity in odd and even numbered cells can be calculated from the solution of Eq. (9).

In the absence of local coupling, where only the long range diffusible signals are acting on the system, there is no bifurcation point and no spatial derivative terms in the continuum equation. The continuum approximation in this case is:

$$M(x,t;\delta) = \lambda g(w) + \delta^2\Lambda g'(w)W(x) \tag{13}$$

$$N(x,t;\delta) = w + \delta^2 W(x) \tag{14}$$

2D Continuum PDE: Following the same procedure as for 1D, we derived an approximate PDE for patterning in a 2D array where one cell has four neighboring cells. The long range EGF and Wnt signals are now:

$$\begin{aligned} E &= e + \delta^2 E(x,y) \\ W &= w + \delta^2 W(x,y) \end{aligned}$$

As discussed in Supplementary Information (Section S4), the 2D PDE is given by:

$$\rho\frac{\partial N_1^+}{\partial \tau} = \frac{1}{2}\left(\frac{\partial^2 N_1^+}{\partial x^2} + \frac{\partial^2 N_1^+}{\partial y^2}\right) - \phi N_1^+ - \psi\left(N_1^+\right)^3 \tag{15}$$

with ρ, ϕ and ψ defined the same as above.

In the absence of local coupling in the 2D array, the continuum approximation is identical to Eqs. (13) and (14) but with x, y components for the EGF and Wnt signal.

2.3. Parameter values, initial conditions, boundary conditions, and numerical solutions

As a highly abstracted model, specific parameter values can not be derived from experimental data. Where applicable, we use similar parameter values to those found in previous investigations (Collier et al., 1996; O'Dea and King, 2011, 2012). All parameter values and their meanings are listed in Table S2 in the Supplementary Information. For the discrete model, initial conditions were chosen in the basin of attraction for the two stable steady states, to ensure convergence to an alternating pattern. Bifurcation and two parameter continuation diagrams were produced using the software XPPAUT (http://www.math.pitt.edu/bard/xpp/xpp.html). For the PDE model, N_1^+ is set to 0.5 everywhere on the domain for the initial conditions. We assume no-flux boundary conditions for N_1^+ along $x = 0$ and $y = 0$, and assume that it decays to its value at the bifurcation point as $x, y \to \infty$. Solutions to the continuum differential equations were calculated by discretizing in space using second order central differencing with step size of 10^{-2}, and the resulting time-dependent ordinary differential equations were solved using the MATLAB (https://www.mathworks.com/products/matlab.html) solver ode15s.

3. Results

3.1. Multicellular ODE model undergoes a pitchfork bifurcation to produce an alternating pattern of cell fates

To determine when the discrete model can exhibit an alternating spatial pattern of cell fates with neighboring cells taking on different steady state expression levels, we investigate the bifurcation dynamics of the discrete model (Eqs. (3)–(4)). Similar to the analysis performed in Collier et al. (1996), O'Dea and King (2011) and O'Dea and King (2012), we consider an array of two cells with periodic boundary conditions in the presence of spatially homogeneous long range signals ($E_i = E, W_i = W$). This results in the simplified system of equations:

$$\frac{dN_1}{dt} = Wf(M_2) - N_1, \qquad \frac{dN_2}{dt} = Wf(M_1) - N_2 \tag{16}$$

$$\frac{dM_1}{dt} = \gamma(\lambda g(N_1) - M_1), \qquad \frac{dM_2}{dt} = \gamma(\lambda g(N_2) - M_2) \tag{17}$$

This system has the homogeneous steady state:

$$N^* = Wf(\lambda g(N^*)) \tag{18}$$

$$M^* = \lambda g(N^*) \tag{19}$$

where N^* denotes the steady state of Notch activity and M^* denotes the steady state of MAPK activity. The Jacobian of this four variable system has the eigenvalues:

$$\epsilon_1 = \frac{-1-\gamma+\sqrt{(1-\gamma)^2+4W\gamma\lambda f'(M^*)g'(N^*)}}{2}$$

$$\epsilon_2 = \frac{-1-\gamma+\sqrt{(1-\gamma)^2-4W\gamma\lambda f'(M^*)g'(N^*)}}{2}$$

$$\epsilon_3 = \frac{-1-\gamma-\sqrt{(1-\gamma)^2+4W\gamma\lambda f'(M^*)g'(N^*)}}{2}$$

$$\epsilon_4 = \frac{-1-\gamma-\sqrt{(1-\gamma)^2-4W\gamma\lambda f'(M^*)g'(N^*)}}{2}$$

By our assumptions on f and g, $\epsilon_{2,4}$ must be real valued. To exclude oscillatory solutions, we require that $(1-\gamma)^2 > -4W\gamma\lambda f'(M^*)g'(N^*) \geqslant 0$ making $\epsilon_{1,3}$ strictly real. Under those conditions, only ϵ_2 is capable of changing sign, and the bifurcation dynamics of the system depend only on ϵ_2. Thus, the bifurcation point occurs when

$$\epsilon_2 = 0 \Rightarrow E = -\left(\frac{\mu+1}{Wf'(M^*)g'(N^*)} + \mu W\right) \tag{20}$$

For our specific choices of f, g (Eqs. (5), (6)), the system exhibits a supercritical pitchfork bifurcation as either long range signal (EGF or Wnt) increases away from zero (Fig. 2). For values of EGF or Wnt above the bifurcation point, we have coexistence of two distinct stable steady states, meaning that in this simplified two cell geometry, each cell takes on a different steady state (Fig. 2C). Which cell takes on the high MAPK/low Notch (1°) steady state and which takes on the low MAPK/high Notch (2°) steady state depends on initial conditions. When we consider a larger array of cells, we find an identical bifurcation condition in the presence of spatially homogeneous EGF and Wnt signals, provided the pattern repeats over an even number of cells. Details of the linear stability analysis and associated eigenvalues for an arbitrary number of cells can be found in the Supplementary Information (Section S2).

As the EGF signal increases while the Wnt signal is held constant, the model undergoes a second bifurcation leading to a loss of distinct steady states in the two cell system (Fig. 2A). In contrast, there is no loss of bistability as the Wnt signal is increased while EGF is held constant (Fig. 2B). This suggests that high levels of EGF signal (that inputs at only one node of the network to enhance MAPK activity) can overwhelm the local Notch signaling to prevent the cells from adopting different levels of MAPK and Notch activity. High levels of Wnt signal, which enhances both MAPK and Notch activity, does not prevent an alternating pattern.

3.2. Weaker local coupling can be compensated for by stronger EGF and Wnt signals in the discrete multicellular model

Local coupling is required for the two cell model to undergo a bifurcation and produce an alternating pattern of cell fates. However, it is not clear how sensitive the bifurcation dynamics are to the strength of local coupling. In particular, we wished to determine whether decreasing the local coupling affects the minimum EGF and Wnt signals required for the model to undergo a pitchfork bifurcation and produce an alternating pattern. This is motivated by experiments that indicate two Caenorhabditis species, *C. elegans* and *C. briggsae*, respond differently to disruption of EGF signaling. In particular, inhibition of MAPK activity in *C. elegans* results in animals without the ability to produce alternating primary and secondary cells, whereas *C. briggsae* animals continue to produce the pattern under similar conditions (Dawes et al., 2017). We simulated this effect in the model by impairing (but not abolishing) local signaling, weakening the ability of MAPK activity to induce Notch activity in neighboring cells. Considering the level of EGF signal required for patterning (the bifurcation point where one steady state transitions to three), when the local signaling from MAPK to Notch is impaired, a stronger EGF signal is needed to ensure patterning (Fig. 3A, red line).

The two parameter continuation diagram (Fig. 3B) summarizes the bifurcation dynamics when EGF and Wnt signals are varied simultaneously. Combined values of EGF and Wnt signals that lie below the black line are not sufficient to induce patterning, while values that lie above the line result in an alternating pattern, and each point along the curve indicates the EGF and Wnt values at the bifurcation point. In the absence of EGF signaling ($x = 0$ in Fig. 3B), a sufficiently high level of Wnt signaling is still capable of inducing an alternating pattern. In the absence of Wnt signaling ($y = 0$), EGF alone is not capable of inducing an alternating pattern. This requirement for Wnt signaling but not EGF likely reflects the distinct nature of the two signals in our model. EGF acts only on MAPK so that high levels of EGF can dominate any Notch activity, abolishing an alternating pattern. In contrast, Wnt acts on both MAPK and Notch independently, balancing the activity of both pathways, allowing an alternating pattern to emerge. This suggests the presence of a threshold in the Wnt signal required for an alternating pattern. This also suggests that systems whose parameter values place them close to the bifurcation line are able to pattern under normal conditions, but quickly lose their ability to pattern in response to small losses in long range (EGF or Wnt) signal strength. In contrast, systems whose parameter values place them further from the bifurcation line are able to continue generating an alternating pattern despite small reductions in the long range EGF and Wnt signals. We can interpret the response of the related nematode worms *C. elegans* and *C. briggsae* to small reductions in MAPK activity (Dawes et al., 2017). The rapid loss of patterning in *C. elegans* suggests this species inhabits a region of parameter space close to the bifurcation line while *C. briggsae* inhabits a region further from the bifurcation line allowing it to continue patterning.

We next investigated the bifurcation dynamics in the two parameter continuation diagram for larger ranges of EGF and Wnt signals (Fig. 4). In the presence of weak local coupling ($\beta \approx 0$), a system can produce an alternating pattern, but requires increasingly higher levels of the EGF and Wnt long range signals (Fig. 4A). As the local coupling strength increases (large β), the difference between the two parameter continuation curves in Fig. 4A becomes smaller, suggesting the presence of local signaling is more important than the magnitude of that interaction. As the level of

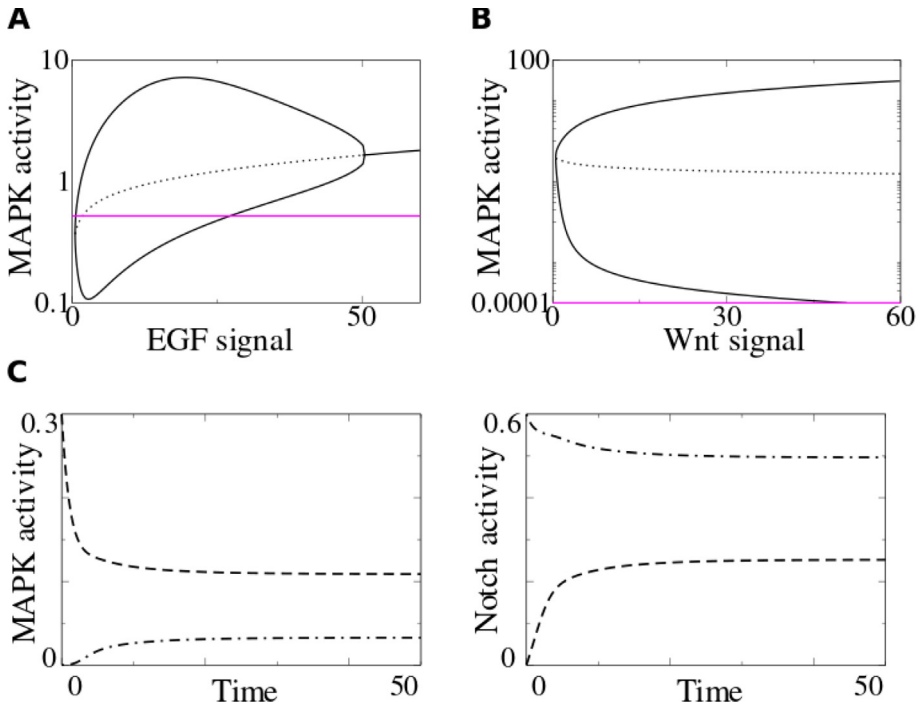

Fig. 2. Bifurcation dynamics of the simplified two cell model. In the presence of local coupling (Eqs. (16), (17)), the equations of the simplified network (Fig. 1B) undergo a supercritical pitchfork bifurcation (black lines) at low values of the long range signal (A: EGF or B: Wnt) (see Fig. 3). Solid black lines indicate stable steady states, dotted black lines indicate unstable steady states. For ease of visualization, the MAPK activity levels are plotted on a log scale. For EGF or Wnt signal values above the bifurcation point, the model exhibits alternating cell fates, with one cell having high MAPK activity (1° cell fate; upper branch of stable steady states) and the other having low MAPK activity (2° cell fate; lower branch). A: Bistability is lost as the EGF signal is increased. B: In contrast, the model continues to produce an alternating cell fate pattern even in the presence of a strong Wnt signal. In the absence of local coupling (Eq. (7)–(8), magenta lines), there is no bifurcation and thus no bistability or alternating pattern in the two cell system. C: Time course of MAPK and Notch activity for EGF and Wnt values above the bifurcation point. One cell (dashed line) takes on high MAPK/low Notch levels (1° cell fate), the other cell (dash-dot line) takes on low MAPK/high Notch levels (2° cell fate).

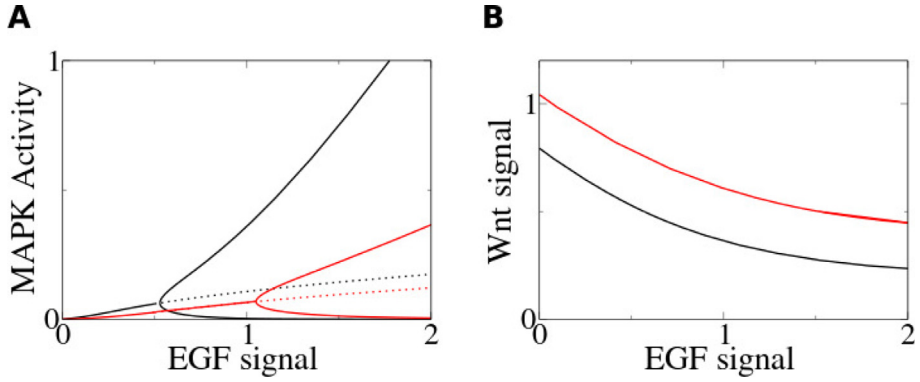

Fig. 3. Dependence of bifurcation dynamics on local coupling strength. A: With default parameter values, the two cell model (Eqs. (16), (17)) undergoes a pitchfork bifurcation as the level of EGF signal increases, transitioning from a single stable steady state (solid black line) to a pair of distinct stable steady states separated by an unstable steady state (dotted black line). When the strength of local coupling is decreased (mediated by MAPK signaling to Notch activity in neighboring cells and represented by parameter β in Eq. (6)), more EGF is needed for the model to undergo the bifurcation (solid and dotted red lines show steady states with 70% decrease in β). B: Two parameter continuation diagram showing combined EGF and Wnt signals required for the model to undergo a bifurcation, with each point along the curve indicating the EGF and Wnt values where the system transitions from one steady state (EGF and Wnt values below the curve) to three steady states (EGF and Wnt values above the curve). With the default parameter set (black line), the external EGF and Wnt signals can combine and compensate for each other to ensure the model undergoes a bifurcation and produces an alternating pattern. When the local coupling is impaired (red line), the bifurcation curve is shifted indicating higher levels of EGF and Wnt are needed for the model undergo a bifurcation.

long range EGF signal increases (moving to the right along the x axis in Fig. 4A), a higher level of Wnt signal is required to produce an alternating pattern. This suggests that high levels of the long range EGF signal can overpower local signaling to activate the MAPK pathway in neighboring cells, abolishing the alternating pattern. High long range Wnt signaling can balance the activity of high EGF, activating local signaling through the Notch pathway and restoring an alternating pattern. No compensation mechanism is required when the long range Wnt signal is increased: the model continues to produce alternating patterns even in the presence of high Wnt signal.

From these extended two parameter continuation diagrams, we note a minimum level of EGF and Wnt signaling required for patterning in the presence of a given local signal strength, β. As described in the Supplementary Information, we can identify general conditions for this minimum. Only one eigenvalue, ϵ_2, is

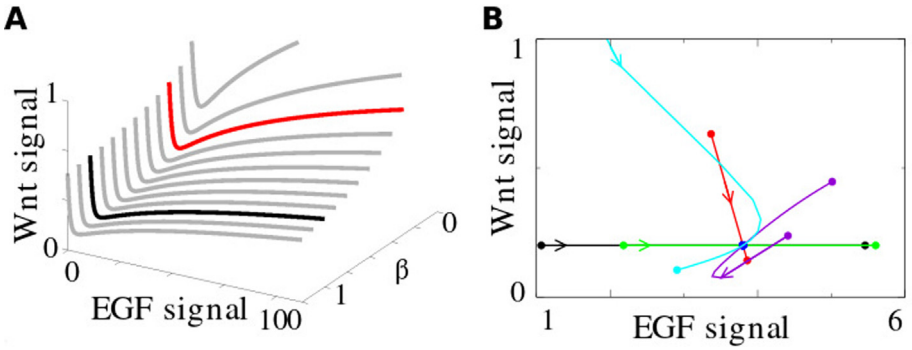

Fig. 4. Minimum EGF and Wnt signaling needed to produce an alternating pattern depends on model parameters. A: Extending the two parameter continuation diagram to higher values of EGF signal and varying local coupling strengths (parameter β in Eq. (6)) indicates minimum combined values of EGF and Wnt signals to produce an alternating pattern. An implicit equation for the minimum of the two parameter curve can be derived (Eq. S33). B: The value of EGF and Wnt at this minimum depends nonlinearly on model parameters (Eqs. (16), (17); Black: α, Red: β, Green: μ, Blue: γ, Cyan: h, Magenta: k). Parameters were varied from 10% to 200% of their default values (Table S2), with the arrow head indicating the direction of increase for each curve.

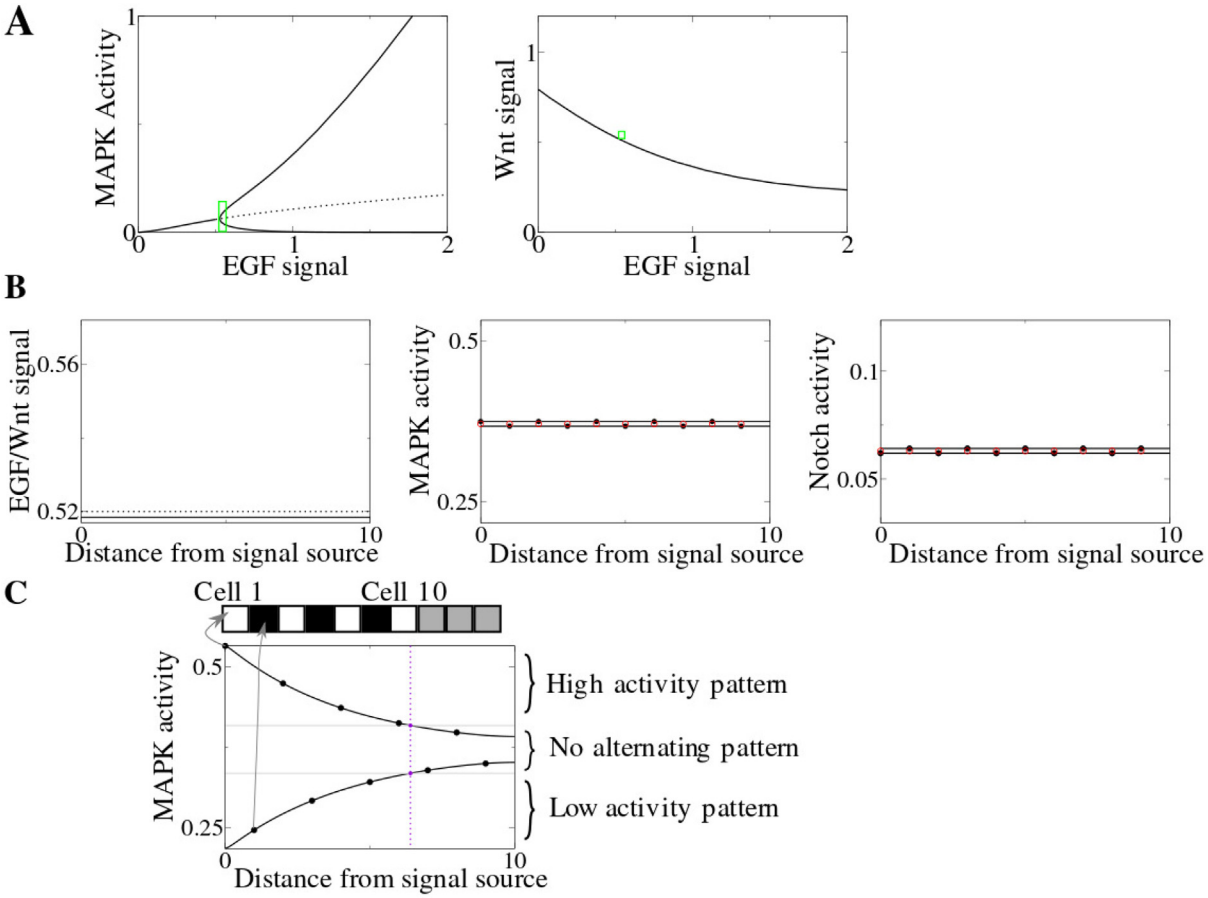

Fig. 5. Continuum PDE approximates dynamics close to the bifurcation point. A: A continuum PDE (Eq. (9)) is derived to investigate the dynamics of the model for small ranges of EGF and Wnt signal values just above the bifurcation point (green boxes). See Fig. 2 and 3 for more detailed bifurcation dynamics. B: For homogeneous EGF (solid black line) and Wnt (dotted black line) signals at their bifurcation values (left), the continuum PDE (black lines) for MAPK (middle) and Notch (right) activity agrees closely with the multicellular model (Eq. (3), (4); red circles). Black dots indicate the midpoint of a cell, for ease of comparison to the discrete model. The y-axis range is chosen to be consistent with Fig. 6. The limited y-axis range is to ensure the continuum approximation is valid. The x-axis indicates distance from the source of the EGF and Wnt signals, with a unit of measurement representing one cell width. C: MAPK activity when EGF and Wnt signals are not spatially homogeneous and have been elevated above their bifurcation values at the signal source (Fig. 6, bottom). The continuum PDE has high and low activity variables. 1° cells have high MAPK (upper solution curve in C)/low Notch activity while 2° cells have low MAPK (lower solution curve in C)/high Notch activity. See Fig. 6 for corresponding Notch activity plots. Light gray horizontal lines indicate values of MAPK activity $\pm 10\%$ from the bifurcation value. Continuum PDE solutions that lie above/below the gray lines are assumed to exhibit an alternating pattern, while solutions that are within 10% of the bifurcation value are assumed to not display any visible patterning. The vertical dotted magenta line indicates the spatial extent of the alternating pattern, where the upper and lower solutions fall within 10% of the bifurcation value. The spatial extent of the pattern does not depend on the number of cells included in the simulation. We choose the x-axis to span 10 cells to optimize data presentation. The extent of visible patterning is visualized in a 1D discrete array and evaluated according to a representative cell position (black dot). White: 1° cells, Black: 2° cells. Dark Gray: unpatterned cells.

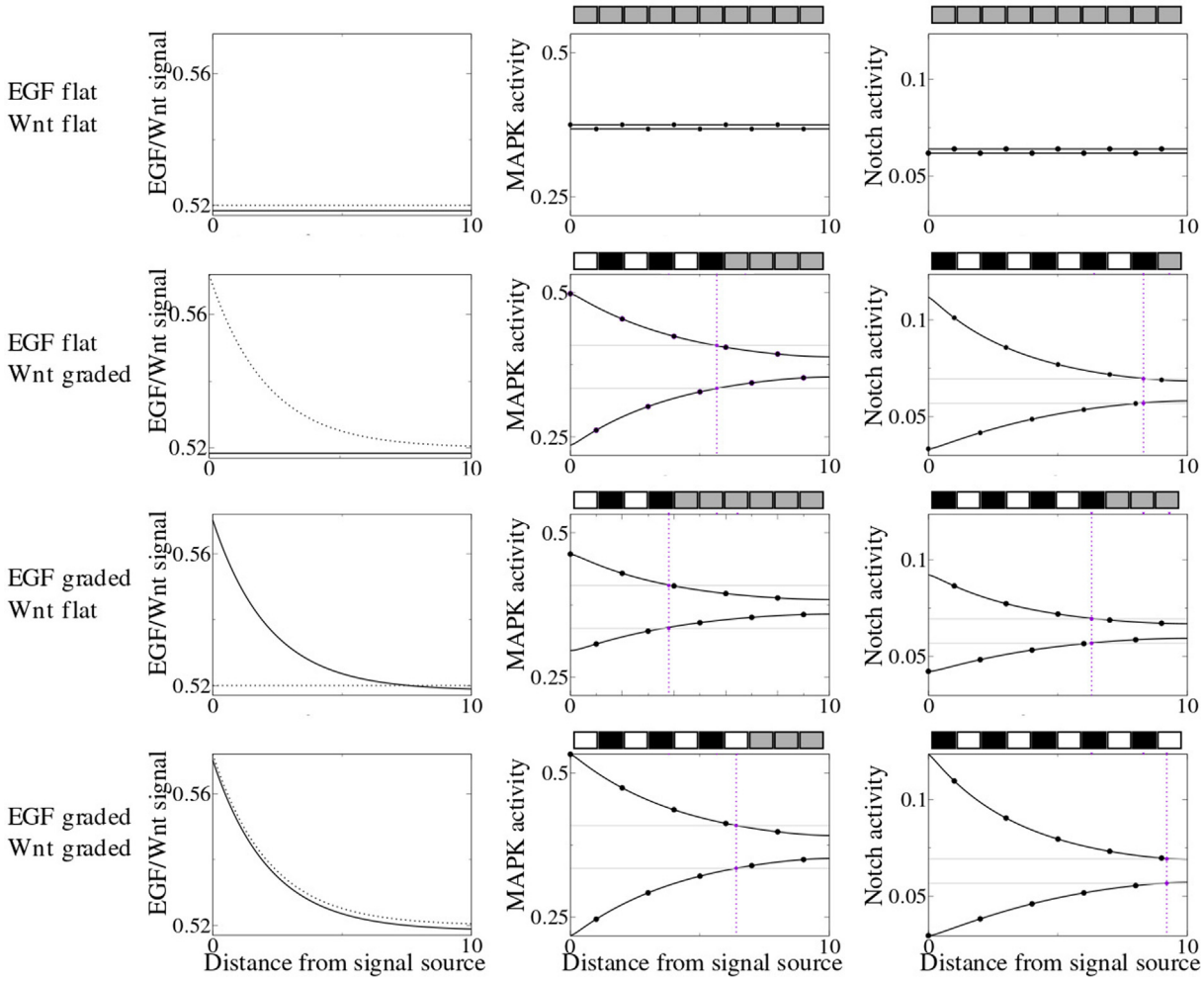

Fig. 6. Continuum PDE solutions for MAPK and Notch dynamics in a 1D array of cells shows patterning further from the signal source when both EGF and Wnt signals are elevated. Spatial profiles of (middle) MAPK and (right) Notch solutions to the continuum PDE (Eq. (9)) in response to different (left) EGF (solid black line) and Wnt (dotted black line) long range signals. The long range EGF and Wnt signals were initially raised to 10% above their bifurcation values at the signal source ($x = 0$) and decay away from the source according to an exponential function. The same decay coefficient was used for both signals. Despite the same spatial decay rates for EGF (solid line) and Wnt (dotted line) long range signals, the presence of both signals allows patterning to extend further into the domain when compared to either signal alone. Dashed purple lines indicate the spatial extend of the alternating pattern, where the MAPK or Notch activity falls to $\pm 10\%$ of the activity level at the bifurcation point (horizontal gray lines). A discrete representation of the visible pattern is shown above each plot, with one unit of measurement on the x-axis representing one cell width. See Fig. 5 for more details on plot components.

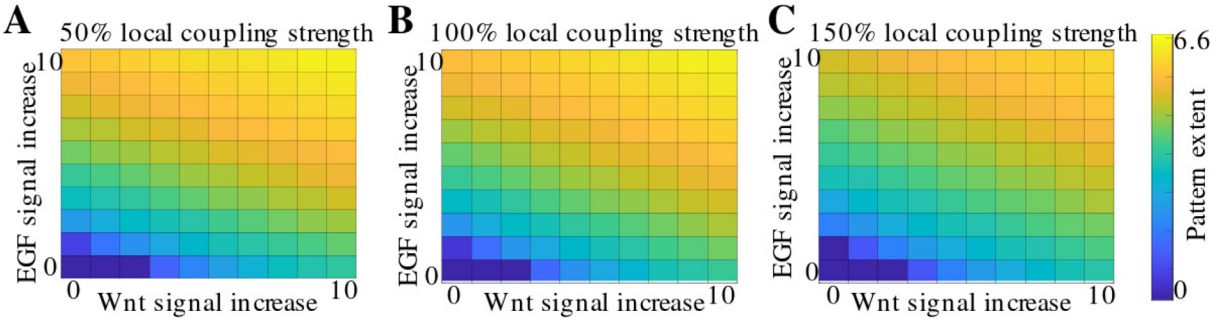

Fig. 7. Local coupling strength does not strongly influence the extent of spatial patterning of the continuum PDE when the rate of spatial EGF and Wnt signaling is held constant. Heat maps show the spatial position where MAPK activity falls to within $\pm 10\%$ of its baseline bifurcation value in response to varying amplitudes of the long range EGF and Wnt signals and local coupling strength, β. This distance is represented by the magenta lines in Fig. 5C. Values on the corresponding axes indicate the percentage increase of the signal above its bifurcation value at the signal source. The spatial decay value is held constant while the local coupling strength β is varied by $\pm 50\%$. Stronger EGF or Wnt signals allow patterning to extend further into the domain, while the local coupling strength has little effect on the spatial extent of the pattern. In all cases where β is varied, a linear relationship between the EGF and Wnt amplitude determines the spatial extent of the patterning. The color bar indicates the spatial extent of the alternating pattern using one cell as a unit of measurement.

capable of changing sign, meaning that ϵ_2 alone determines the position of the bifurcation point. For a given local coupling strength β, we designate the curve corresponding to $\epsilon_2 = 0$ in the two parameter continuation diagram as the function $W(E)$. With the requirement that the interaction functions f, g are monotonically increasing/decreasing respectively, we find $W(E)$ has a minimum when Eq. S33 (Supplementary Information) is satisfied. In other words, for a given local coupling strength β, there is an optimal condition under which the system can minimize the amount of long range EGF and Wnt signals while ensuring the presence of an alternating pattern. The values of EGF and Wnt signal associated with this minimum are sensitive to most model parameters (Fig. 4B). As expected, the parameter γ, which dictates the time scale of MAPK activity (Eq. (4)), has no effect on the position of the minimum. Two parameters, α which is the half maximum value in the local coupling function Eq. (5) and μ which is the relative contribution of the Wnt signal to MAPK activity (Eq. (4)), only influence the level of EGF signal associated with the minimum. The remaining parameters, β which is the half maximum value of the function Eq. (6), as well as k and h, the degree of cooperativity in the coupling functions Eqs. (5), (6), influence both the EGF and Wnt levels associated with the minimum levels needed for patterning. This suggests that altered model parameters can compensate for changes in long range EGF or Wnt signals, preserving a system with an alternating pattern Supplementary Information (Section S3).

3.3. Continuum approximation of multicellular model captures dynamics around the bifurcation point

Cells can be highly responsive to inputs, suggesting that dynamics close to the bifurcation point are especially important. To study the dynamics of the model close to the bifurcation point determined above (Fig. 5A), we follow the multiscale method in O'Dea and King (2011, 2012) and derive a continuum PDE centered at the bifurcation point, Eq. (20), that explicitly incorporates short and long range signals. This continuum PDE not only allows us to study the dynamics of the model in response to small amplitude perturbations, it also provides a continuum approximation of our multicellular model, Eqs. (3)–(4). As detailed in Supplementary Information, the continuum PDE retains terms to third order, providing reasonable agreement to the full multicellular model (Fig. 5B). This continuum approximation is only valid when the EGF and Wnt signal levels are varied by small amounts, and this small variation is reflected in the limited y-axis ranges in Figs. 5, 6, and 8. By incorporating the alternating nature of the pattern

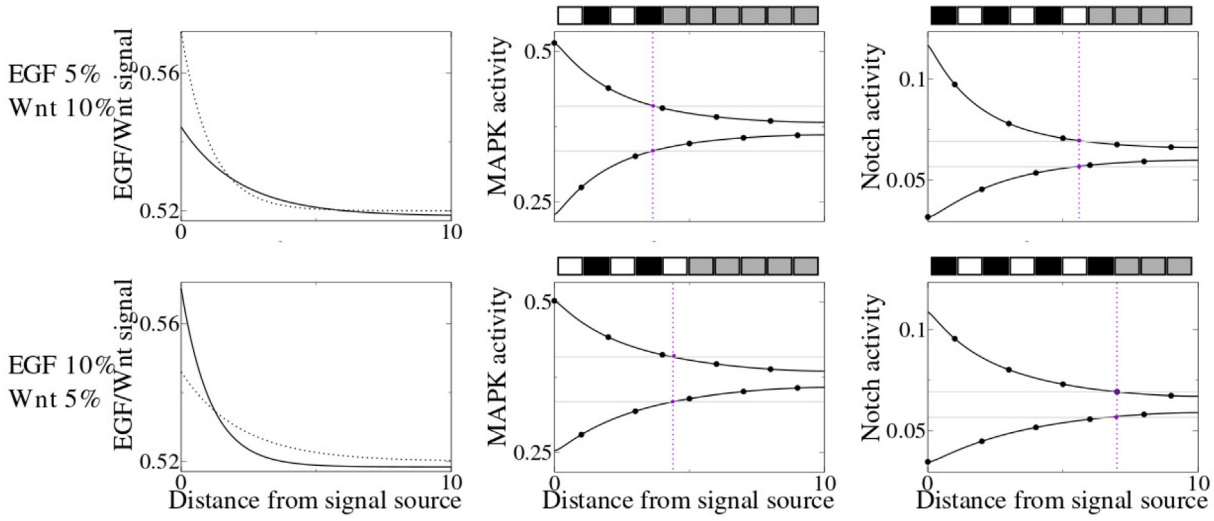

Fig. 8. Spatial patterning of the continuum PDE in a 1D cell array extends further in response to an elevated EGF signal compared to Wnt when total signal is conserved. Spatial profiles of (middle) MAPK and (right) Notch solutions to the continuum PDE (Eq. (9)) in response to different (left) EGF and Wnt long range signals. The long range EGF and Wnt signals were raised to 5 or 10% above their bifurcation values at the source of the signal ($x = 0$). The exponential decay coefficient was calculated to conserve the total amount of signal on the domain. The alternating cell fate pattern extends further away from the signal source when EGF is raised to 10% above its bifurcation level, compared to a similar increase in the Wnt signal. See Fig. 5 for more details on plot components.

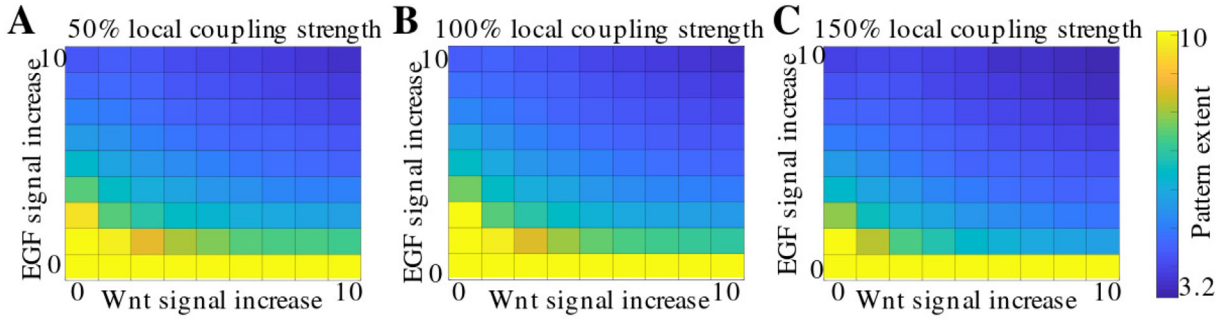

Fig. 9. Local coupling strength does not strongly influence the extent of spatial patterning of the continuum PDE when total signal but not spatial decay is conserved. Heat maps show the spatial position where MAPK activity of the continuum PDE (Eq. (9)) falls to within ±10% of its baseline bifurcation value in response to varying initial amplitudes of the long range EGF and Wnt signals and local coupling strength, β. Here, the spatial decay coefficient is calculated to conserve the total amount of signal over the domain. Consistent with Fig. 8, the strength of local coupling does not strongly influence the spatial extent of the alternating pattern. The color bar indicates the spatial extent of the alternating pattern using one cell as a unit of measurement.

generated by the pitchfork bifurcation, the continuum PDE directly relates to patterning in the discrete multicellular system, and we can visualize the alternating pattern in a discrete cell array (Fig. 5C).

3.4. Spatial extent of alternating pattern in 1D continuum PDE model depends on EGF and Wnt signal amplitude but not local coupling strength

With the continuum PDE, we first investigated the spatial extent of an alternating pattern in response to small spatial perturbations to the long range diffusible signal. These perturbations result in the height (amplitude) of the EGF and/or Wnt signal being elevated above its bifurcation value by up to 10% at the signal source. The long range signal is assumed to originate from the anchor cell, which is positioned at $x = 0$. We assume the long range signal obeys a simple reaction–diffusion equation and therefore decays exponentially away from the source. When the spatial decay rate is held constant while the amplitude of the long range signal at its source is increased, meaning the model does not receive any additional spatial information from the signal, the alternating pattern extends further into the domain (Fig. 6). Consistent with the discrete multicellular model (Fig. 4), the spatial extent of the alternating pattern in response to the same EGF and Wnt signals is largely independent of the local coupling strength, corresponding to a change in the parameter β (Fig. 7). To ensure a consistent comparison, the same domain size was used for each simulation.

When the spatial decay is held constant, the alternating pattern extends further into the domain in the presence of elevated Wnt signal compared to a similar elevation in the EGF signal (Fig. 6). While there is no additional spatial information in this case, the total amount of signal varies as the initial amplitude of the EGF and Wnt signals are varied. To determine if the patterning extent is affected by the total amount of EGF or Wnt signal on the domain, we varied both the initial amplitude as well as the spatial decay so that the total amount of signal on the domain is constant (Fig. 8). In the presence of conserved signal amount, we see that elevated EGF signal results in further spatial patterning compared to a similar increase in Wnt signal. As expected, the extent of spatial patterning is not strongly affected by the strength of local coupling (Fig. 9).

Taken together, this suggests the model is more sensitive to increased Wnt signaling when the spatial decay of the signal is independent of the amount of signal, but is more sensitive to the EGF signal when the total amount of signal is conserved. This may be due to Wnt signaling enhancing both MAPK and Notch activity, so that when spatial decay is fixed, alternating activity can extend further into the domain by communication between neighboring cells.

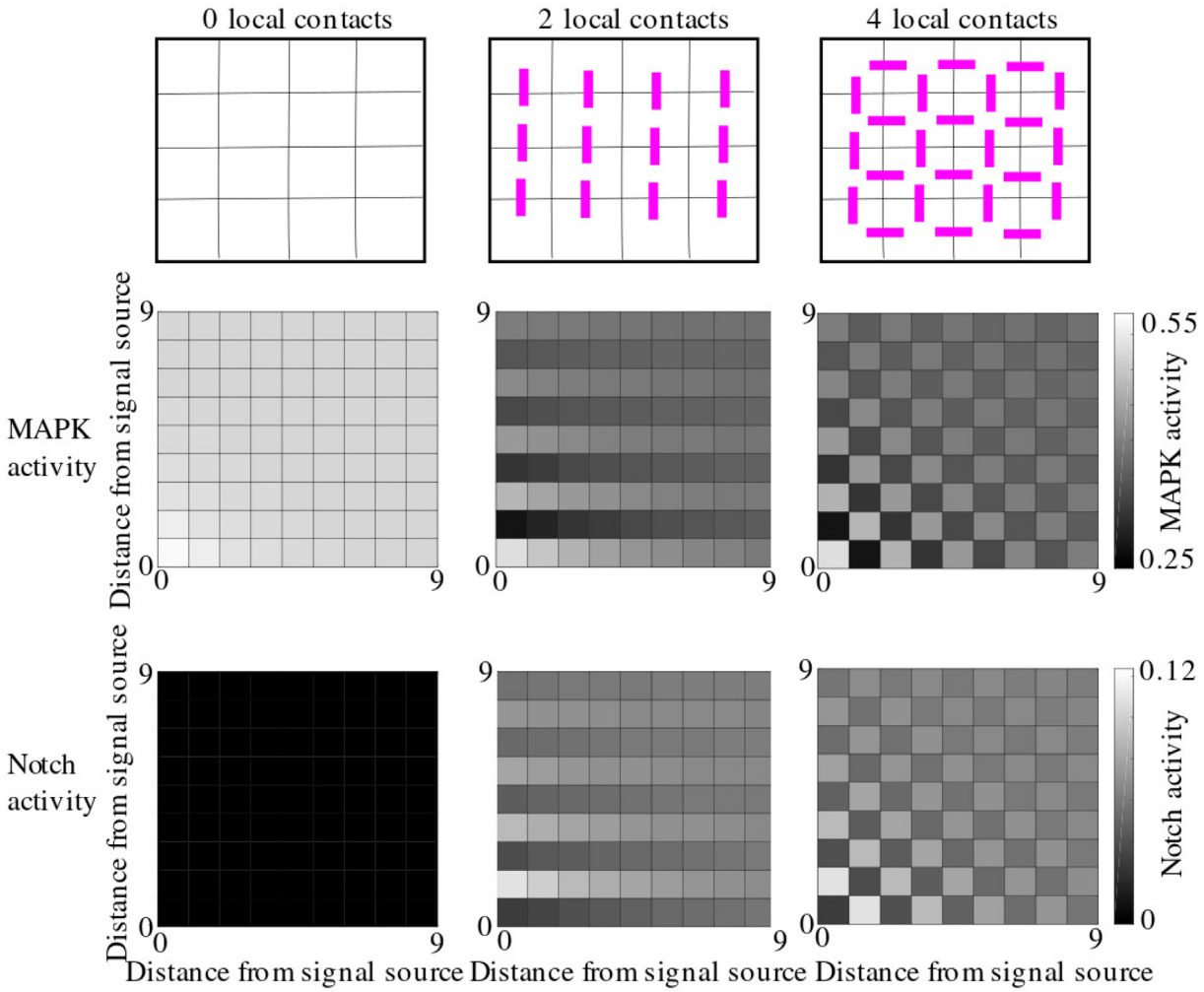

Fig. 10. In a 2D array of cells, local coupling determines the type of pattern in the continuum PDE. MAPK and Notch activity in a 2D domain (Eq. (15)) with local signaling between (left) 0 neighboring cells, (middle) 2 neighboring cells, or (right) 4 neighboring cells. Patterns in the 2D array range from no alternating pattern, a checkerboard pattern, and striped pattern, depending on how neighboring cells communicate via contact-mediated signaling. The upper and lower bounds of the color scale are the same across all three cases of local contacts.

3.5. Type of alternating pattern in 2D continuum PDE model depends on local coupling

After considering the spatial extent of patterning with the 1D continuum model, we wished to investigate the dynamics of the continuum model in a 2D domain. We derived and simulated the continuum PDE following a similar method as for the 1D continuum model (Eq. (15) and Supplementary Information, Section S4). The direction of coupling, along with the number of cells connected in the local neighborhood, determine the pattern type exhibited by the model (Fig. 10). With 0 local neighbors connected (no local coupling), there is no pattern, consistent with our bifurcation results above. With two neighboring cells connected in parallel rows, we see a striped pattern with the alternating pattern in the direction of coupling, while local coupling in all directions (four neighbors connected) results in a checkerboard pattern.

When we consider the spatial extent of the pattern along the x or y axes, we see that the type of coupling also dictates the spatial extent of the alternating pattern (Fig. 11). When the coupling is symmetric (0 or 4 neighbors), the pattern (or lack thereof) extends equally along both axes. With asymmetric local coupling (2 neighbors), the pattern extends further in the direction of coupling, extending even further into the domain compared to 4 neighbors, and the pattern drops off more quickly opposite to the direction of coupling at a point closer to the signal source than the 4 neighbor case. This indicates that the extent and type of spatial pattern in an array of cells can be regulated just by changes in local signaling. It also demonstrates that different patterns can be produced by a long range signal when local signaling is present.

4. Discussion

Cells rely on a small number of signaling pathways to regulate cell fate decisions during development (Alberts et al., 2002; Perrimon et al., 2012). Yet arrays of cells are able to generate different complex spatial patterns that lead to proper tissue positioning and cell function in a mature organism. In this study, we analyzed a model for cell fate specification that incorporates both long range diffusible signals (mediated by EGF and Wnt ligands) as well as local contact-mediated signaling (mediated by Notch ligands). While the model is inspired by the relationship among signals important for Caenorhabditis vulval development and investigates patterns that repeat over two cells, coincident utilization of combinations of long-range and local signals to produce pattern is widely deployed in animal development. Examples range from patterning of digits and ribs in vertebrates (Sonnen et al., 2018; Tickle, 2015) and the placement of insect bristles, bird feathers or mammalian hair follicles (Simpson et al., 1999; Crowe et al., 1998; Lin et al., 2009; Rishikaysh et al., 2014), to maintenance in physiological processes such as vascular branching and intestinal cell turn-over (Beumer and Clevers, 2016; Herbert and Stainier, 2011). The methods used here can be extended to investigate patterns that exhibit complex patterns repeating over larger numbers of cells.

Our model identifies an important trade-off in systems using a combination of long-range and local signaling. The model reliably produces an alternating pattern of cell fates in the presence of a sufficiently strong long range signal. However, cellular characteristics may constrain the placement of the system relative to the bifurcation point. Those cells with characteristics that place it closer to the bifurcation point can produce a pattern in response to lower long-range signal levels, but quickly lose the ability to pattern in the presence of perturbations that reduce the long-range signal. Cells further from the bifurcation point produce a higher dose of long-range signals. While the higher dose is more than what is needed to produce a pattern under wild-type conditions, it makes the system more robust to perturbations. Especially in the context of multiple, partially compensatory long-range signals, this feature may be selected for, or allow for considerable develop-

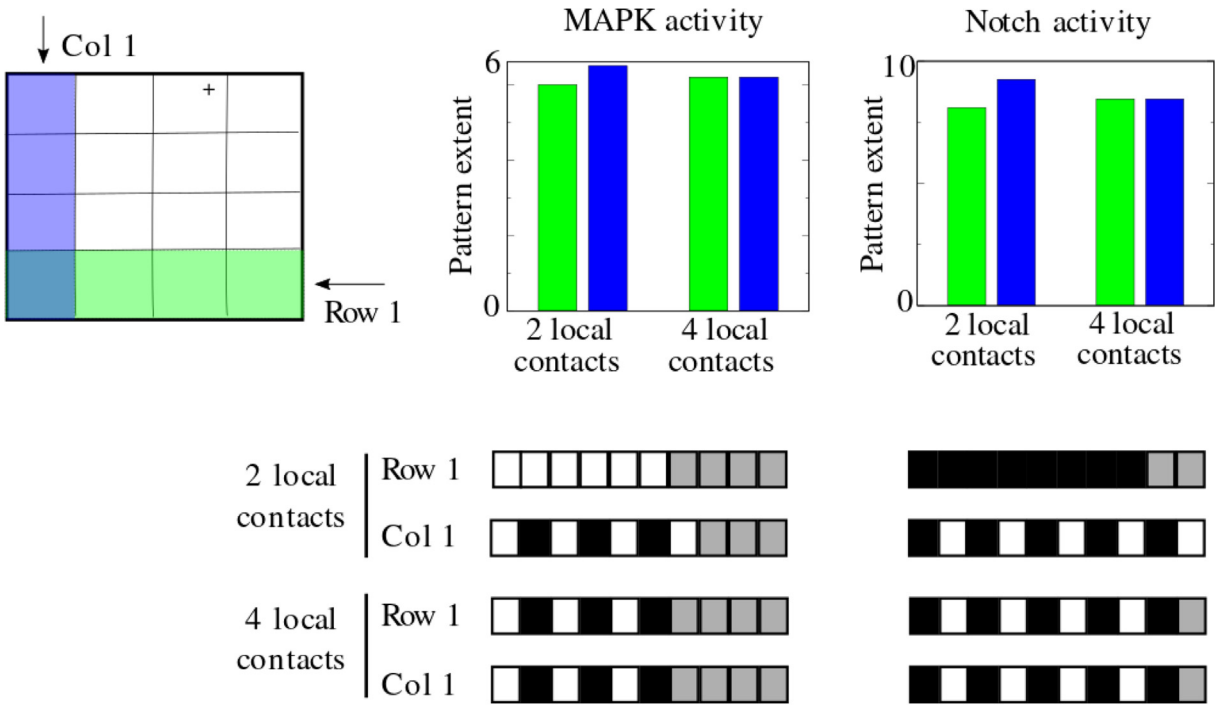

Fig. 11. In a 2D array of cells, local coupling determines the spatial extent of the alternating cell fate pattern in the continuum PDE. MAPK and Notch activity along the first row or first column in a 2D domain (Eq. (15)). With symmetric coupling (4 neighboring cells) the pattern extends equally in the x and y directions. With asymmetric coupling (2 neighboring cells), the pattern extends further in the direction of coupling (column 1) as compared to the model values orthogonal to the direction of coupling (row 1). (Bottom) The extent of the pattern along the first row or column is illustrated. White/black indicates activity levels at least 10% above/below the steady state value, gray indicates activity levels within 10% of steady state vales.

mental system drift. For example, genetic experiments show that the critical signal for vulval development is Wnt in some nematode species, EGF in others, or that both have a role (Hill and Sternberg, 1992; Myers and Greenwald, 2007; Tian et al., 2008; Vargas-Velazquez et al., 2019), consistent with the range of outcomes possible under these constraints.

We derived a continuum PDE model to examine the patterning behavior of cells with dynamics close to the bifurcation point that are therefore most sensitive to the loss of long-range signals. In this model, the spatial extent of a pattern is determined by the amplitude of the long-range signals, and is less dependent on the strength of local coupling. A biological example consistent with this observation is the intestinal crypt, responsible for replenishing cells in the intestine. Both Wnt and Notch function to maintain a checkerboard pattern of stem cells and Paneth cells at the base of the crypt, with Wnt dose important in crypt formation and fate patterning (Hirata et al., 2013, reviewed in Beumer and Clevers, 2016). The continuum PDE model also demonstrates that local coupling is critical for determining the type of spatial pattern generated in an array of cells, with the same system but distinct coupling features yielding either checkerboard or striped patterns. Diptera (fly) species provide a potential biological example in which a directional coupling process to produce rows of bristles on the dorsal mesothorax modulates the ancestral pattern of uniformly spaced (checkerboard) bristles (Simpson et al., 1999). Taken together, the results from this generalizable mathematical framework highlight the distinct but complementary roles played by long range and local signaling in regulating pattern formation during development.

CRediT authorship contribution statement

Carly Williamson: Conceptualization, Methodology, Software, Formal analysis, Writing - original draft, Writing - review & editing. **Helen M. Chamberlin:** Conceptualization, Methodology, Writing - original draft, Writing - review & editing. **Adriana T. Dawes:** Conceptualization, Methodology, Software, Formal analysis, Writing - original draft, Writing - review & editing.

Declaration of Competing Interest

The authors declare that they have no known competing financial interests or personal relationships that could have appeared to influence the work reported in this paper.

Acknowledgments

This work was supported by the NSF grant DMS-1361251 to ATD and HMC. We thank the Dawes and Chamberlin labs for helpful discussions and comments.

Appendix A. Supplementary data

Supplementary data associated with this article can be found, in the online version, athttps://doi.org/10.1016/j.jtbi.2021.110596.

References

Alberts, Bruce, Johnson, Alexander, Lewis, Julian, Raff, Martin, Roberts, Keith, Walter, Peter (Eds.), 2002. Molecular Biology of the Cell. 4th ed. Garland Science, New York.

Beumer, J., Clevers, H., 2016. Regulation and plasticity of intestinal stem cells during homeostasis and regeneration. Development (Cambridge) 143, 3639–3649.

Collier, J.R., Monk, N.A., Maini, P.K., Lewis, J.H., 1996. Pattern formation by lateral inhibition with feedback: a mathematical model of delta-notch intercellular signalling. Journal of Theoretical Biology 183, 429–446.

Crowe, R., Henrique, D., Ish-Horowicz, D., Niswander, L., 1998. A new role for Notch and Delta in cell fate decisions: Patterning the feather array. Development 125, 767–775.

Dawes, A.T., Wu, D., Mahalak, K.K., Zitnik, E.M., Kravtsova, N., Su, H., Chamberlin, H. M., 2017. A computational model predicts genetic nodes that allow switching between species-specific responses in a conserved signaling network. Integrative Biology 9, 156–166.

De Back, W., Zhou, J.X., Brusch, L., 2013. On the role of lateral stabilization during early patterning in the pancreas. Journal of the Royal Society Interface 10.

Erkenbrack, E.M., 2018. Notch-mediated lateral inhibition is an evolutionarily conserved mechanism patterning the ectoderm in echinoids. Development Genes and Evolution 228.

Fisher, J., Piterman, N., Hubbard, E.J.A., Stern, M.J., Harel, D., 2005. Computational insights into Caenorhabditis elegans vulval development. Proceedings of the National Academy of Sciences of the United States of America 102, 1951–1956.

Giurumescu, C.A., 2006. Intercellular coupling amplifies fate segregation during Caenorhabditis elegans vulval development. In: Proceedings of the National Academy of Sciences 103.

Greenwald, I.S., Sternberg, P.W., Horvitz, H.R., 1983. The lin-12 locus specifies cell fates in Caenorhabditis elegans. Cell 34, 435–444.

Han, M., Aroian, R.V., Sternberg, P.W., 1990. The let-60 locus controls the switch between vulval and nonvulval cell fates in Caenorhabditis elegans. Genetics 3, 899–913.

Herbert, S.P., Stainier, D.Y., 2011. Molecular control of endothelial cell behaviour during blood vessel morphogenesis. Nature Reviews Molecular Cell Biology 12, 551–564.

Hill, R.J.J., Sternberg, P.W.W., 1992. The gene lin-3 encodes an inductive signal for vulval development. Nature 358, 470–476.

Hirata, A., Utikal, J., Yamashita, S., Aoki, H., Watanabe, A., Yamamoto, T., Okano, H., Bardeesy, N., Kunisada, T., Ushijima, T., Hara, A., Jaenisch, R., Hochedlinger, K., Yamada, Y., 2013. Dose-dependent roles for canonical Wnt signalling in de novo crypt formation and cell cycle properties of the colonic epithelium. Development (Cambridge) 140, 66–75.

Irons, D.J., Wojcinski, A., Glise, B., Monk, N.A., 2010. Robustness of positional specification by the Hedgehog morphogen gradient. Developmental Biology 342, 180–193.

Lin, C.M., Jiang, T.X., Baker, R.E., Maini, P.K., Widelitz, R.B., Chuong, C.M., 2009. Spots and stripes: Pleomorphic patterning of stem cells via p-ERK-dependent cell chemotaxis shown by feather morphogenesis and mathematical simulation. Developmental Biology 334, 369–382.

Myers, T.R., Greenwald, I., 2007. Wnt signal from multiple tissues and lin-3/EGF signal from the gonad maintain vulval precursor cell competence in Caenorhabditis elegans. Proceedings of the National Academy of Sciences of the United States of America 104, 20368–20373.

O'Dea, R.D., King, J.R., 2011. Multiscale analysis of pattern formation via intercellular signalling. Mathematical Biosciences 231, 172–185.

O'Dea, R.D., King, J.R., 2012. Continuum limits of pattern formation in hexagonal-cell monolayers. Journal of Mathematical Biology 64, 579–610.

Pandey, A., Harvey, B.M., Lopez, M.F., Ito, A., Haltiwanger, R.S., Jafar-Nejad, H., 2019. Glycosylation of specific notch EGF repeats by O-Fut1 and fringe regulates notch signaling in drosophila. Cell Reports 29, 2054–2066.e6.

Perrimon, N., Pitsouli, C., Shilo, B.Z., 2012. Signaling mechanisms controlling cell fate and embryonic patterning. Cold Spring Harbor perspectives in biology 4, a005975.

Rishikaysh, P., Dev, K., Diaz, D., Qureshi, W., Filip, S., Mokry, J., 2014. signaling involved in hair follicle morphogenesis and development. International Journal of Molecular Sciences 15, 1647–1670.

Romero-Carvajal, A., Navajas Acedo, J., Jiang, L., Kozlovskaja-Gumbriene, A., Alexander, R., Li, H., Piotrowski, T., 2015. Regeneration of sensory hair cells requires localized interactions between the notch and Wnt pathways. Developmental Cell 34, 267–282.

Simpson, P., Woehl, R., Usui, K., 1999. The development and evolution of bristle patterns in Diptera. Development 126, 1349–1364.

Sonnen, K.F., Lauschke, V.M., Uraji, J., Falk, H.J., Petersen, Y., Funk, M.C., Beaupeux, M., François, P., Merten, C.A., Aulehla, A., 2018. Modulation of phase shift between Wnt and notch signaling oscillations controls mesoderm segmentation. Cell 172, 1079–1090.e12.

Sternberg, P.W., 1988. Lateral inhibition during vulval induction in Caenorhabditis elegans. Nature 335, 551–554.

Sternberg, P.W., 2005. Vulval development. WormBook: The Online Review of C. elegans Biology, 1–28..

Sternberg, P.W., Horvitz, H.R., 1989. The combined action of two intercellular signaling pathways specifies three cell fates during vulval induction in C. elegans. Cell 58, 679–693.

Tian, H., Schlager, B., Xiao, H., Sommer, R.J., 2008. Wnt Signaling Induces Vulva Development in the Nematode Pristionchus pacificus. Current Biology 18, 142–146.

Tickle, C., 2015. How the embryo makes a limb: Determination, polarity and identity. Journal of Anatomy 227, 418–430.

Tiedemann, H.B., Schneltzer, E., Beckers, J., Przemeck, G.K., Hrabě de Angelis, M., 2017. Modeling coexistence of oscillation and Delta/Notch-mediated lateral inhibition in pancreas development and neurogenesis. Journal of Theoretical Biology 430, 32–44.

Vargas-Velazquez, A.M., Besnard, F., Félix, M.A., 2019. Necessity and contingency in developmental genetic screens: EGF, Wnt, and semaphorin pathways in vulval induction of the nematode oscheius tipulae. Genetics 211, 1315–1330.